Permeation of Aromatic Carboxylic Acids across Lipid Bilayers: The pH-Partition Hypothesis Revisited

Anita V. Thomae, Heidi Wunderli-Allenspach, and Stefanie D. Krämer
Department of Chemistry and Applied Biosciences, ETH Federal Institute of Technology, 8093 Zurich, Switzerland

ABSTRACT According to the pH-partition hypothesis the charged species of organic compounds do not contribute to lipid bilayer permeation as they generally show negligible partitioning into *n*-octanol. With this assumption, membrane permeation is related to the molar fraction of the neutral species at a particular pH. A recently developed permeation assay permits us to directly determine pH-dependent permeation of aromatic carboxylic acids. Tb^{3+}-loaded liposomes are incubated with aromatic carboxylic acids and upon excitation at the absorption wavelength of the acid, permeation kinetics can be measured as an increase in Tb^{3+} luminescence. The anions of the tested acids permeated egg phosphatidylcholine membranes only 12 (2-hydroxynicotinic acid), 66 (salicylic acid), and 155 (dipicolinic acid) times slower than the net neutral species. The anions, therefore, controlled the total permeation already at 1–2 pH units above their pK_a. These results indicate that in contrast to the expectations of the pH-partition hypothesis, lipid bilayer permeation of an acidic compound can be completely controlled by the anion at physiological pH.

INTRODUCTION

Drug discovery aims at predicting and controlling the permeation of in vivo barriers as early as possible during lead finding and drug optimization to minimize failures in later development (1–3). The major objectives are to overcome epithelial and endothelial barriers in the body and to reach possible intracellular targets. Although lipid bilayers play a key role in the regulation of barrier passage, experimental techniques to explore lipid bilayer permeation are not sufficiently established to perform systematic studies on drug-membrane permeation and to explore the quantitative relations between structural features and bilayer permeation (4). Membrane permeation is generally estimated from experimentally derived or structure-related descriptors for the lipophilicity of a compound, such as the *n*-octanol/buffer partition coefficient (5), the affinities to various lipophilic phases determined by chromatographic methods (6), the permeation across lipid/solvent-impregnated filters (7), as well as parameters calculated from the molecular size, hydrogen-bonding capacities, and polarity descriptors (8). Little is known on the relationship between membrane affinity, which can easily be determined (9), and membrane permeation. Neither the influence of the ionization state of the permeant nor the effect of counterions on permeation is well understood. The pH-partition hypothesis is frequently applied to estimate membrane permeation at a particular pH, assuming that only the neutral form of an acid or a base can permeate lipid bilayers (10,11).

Planar lipid bilayers, also called black-lipid membranes, and liposomes are the two most frequently used systems to study bilayer permeation kinetics (4). In the first system, the aqueous compartments on either side of the bilayer are accessible for probing and sampling allowing direct kinetic measurements. However, as the concentrations of the permeant are determined at a distance from the membrane, the unstirred water layer adjacent to the lipid membrane acts as an additional diffusion barrier. Planar lipid bilayers are physically unstable and contain residual solvent molecules. Liposomes have a better physical stability and can be prepared without solvents or other adjuvants. However, in kinetic studies, the luminal aqueous compartment is not accessible for sampling and the distinction between permeation and membrane/water partitioning is not always straightforward. Permeation kinetics with liposomes can directly be measured with fluorescent permeants with quenching characteristics. However, the range of compounds with such properties is relatively small.

We recently developed an assay to study the kinetics of lipid bilayer permeation of aromatic carboxylic acids (ACAs) (12). Tb^{3+}-containing liposomes are incubated with the ACA and the system is excited at a wavelength that is absorbed by the acid. Upon permeation, the ACAs chelate or ligate Tb^{3+} in the liposomal lumen leading to an increase of the Tb^{3+} luminescence due to an energy transfer from the aromatic system to the Tb^{3+} ion. The assay has been successfully used to study the ability of the cell-penetrating peptide TAT(44–57) to permeate lipid bilayers. It furthermore offers the opportunity to gain new insight into the membrane permeation of ACAs.

In this work, the permeation of salicylic acid (SA), 2-hydroxynicotinic acid (2-OH-NA), and dipicolinic acid (DPA; Fig. 1) across phosphatidylcholine (PhC) bilayers

Submitted February 11, 2005, and accepted for publication June 6, 2005.

Address reprint requests to Stefanie D. Krämer, Institute of Pharmaceutical Sciences, ETH, Wolfgang-Pauli-Strasse 10, CH-8093 Zurich, Switzerland. Tel.: +41-44-633-7403; Fax: +41-44-633-1457; E-mail: skraemer@pharma.ethz.ch.

0006-3495/05/09/1802/10 $2.00

doi: 10.1529/biophysj.105.060871

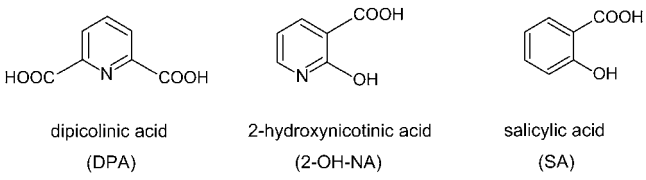

dipicolinic acid (DPA) | 2-hydroxynicotinic acid (2-OH-NA) | salicylic acid (SA)

FIGURE 1 Structures of the studied ACAs.

was studied as a function of pH. As could be demonstrated, the deprotonated ACAs contributed considerably to the permeation, contradicting the pH-partition hypothesis.

MATERIAL AND METHODS

Chemicals

2-OH-NA (No. 55966), 3-(*N*-morpholino) propane sulfonic acid (MOPS, No. 69947), and SA (No. 84210) were purchased from Fluka (Buchs, Switzerland). DPA (No. D0759) was supplied by Sigma (Buchs, Switzerland), and $TbCl_3$ hexahydrate (No. 21290-3) by Aldrich (Buchs, Switzerland). ^{14}C-salicylic acid (No. NEC263) was purchased from PerkinElmer (Boston, MA). For the potentiometric titrations, 0.5 N HCL (No. 1.09971) and 0.5 N KOH (No. 1.09919) Titrisol from Merck (Darmstadt, Germany) were used. Egg PhC grade 1 was supplied by Lipid Products (Nutfield, UK) and di-palmitoyl-PhC (DPPC, No. 850355) from Avanti Polar Lipids (Alabaster, AL). All other chemicals were of analytical grade.

Potentiometric determination of pK_a and $logP_{Octanol}$

The pK_a values of the studied ACAs were determined potentiometrically at 25°C using the PCA 101 instrument from Sirius Analytical Instruments (East Sussex, UK). Titrations were done in triplicates in 0.15 M KCl with 0.5 M HCl and 0.5 M KOH, respectively. The pK_a values were calculated from the titration curves with the pKaLOGP software (Sirius Analytical Instruments). Partition coefficients of the ACAs in *n*-octanol/0.15 M KCl were determined potentiometrically with the same instrument with at least four different volume ratios of organic and aqueous phase between 0.05 and 20 (13). The $logP_{Octanol}$ values were fitted with SigmaPlot 8.0 (SPSS, Chicago, IL) according to Krämer et al. (14).

Preparation of the liposomes

Liposomes were prepared by extrusion (12,15). In brief, for the preparation of Tb^{3+}-containing liposomes, 0.2 mmol $TbCl_3$ hexahydrate and 100 mg lipids were dissolved in methanol and dried to a film in a round flask at least 20 K above the transition temperature (T_c) of the lipids. The film was rehydrated at the same temperature with 2 ml water to form multilamellar liposomes that were subjected to five cycles of freezing and thawing and subsequent extrusion at a temperature $\geq$10 K above T_c of the lipids through double-stacked Nucleopore polycarbonate membranes with an average pore diameter of 200 nm (Corning, Acton, MA). External Tb^{3+} was separated from the liposomes on a Sephadex G-25 PD-10 desalting column (Amersham Biosciences, Freiburg, Germany) with 0.2 M NaCl or water, in the case of permeation experiments with TRIS/HCl. The collected fraction contained ~20–30 mg lipids per ml. The local concentration of Tb^{3+} in the liposomal lumen was between 5 and 7 mM (12). Tb^{3+}-containing liposomes were used within a few hours. Liposomes for partition studies (without Tb^{3+}) were stored at 4°C and used within three days.

Characterization of the liposomes

The average size and the size distribution of all liposome preparations were analyzed by dynamic light scattering with a Zetasizer 3000 HSA (Malvern Instruments, Malvern, UK). Tb^{3+}-containing PhC liposomes showed an average mean hydrodynamic diameter between 140 and 180 nm and Tb^{3+}-free liposomes between 120 and 160 nm. The polydispersity indices of both types of liposomes were <0.2. To rule out the binding or adsorption of Tb^{3+} to the membrane surface, the zetapotential of Tb^{3+}-containing liposomes was determined with the Zetasizer 3000 HSA and compared to Tb^{3+}-free liposomes. Zetapotentials were similar for both preparations, i.e., 5 $\pm$ 4 mV, indicating that Tb^{3+} did not significantly adsorb to the outer surface of the membrane.

Permeation assay

The entry kinetics of the ACAs into the aqueous liposomal lumen containing the Tb^{3+} were determined based on a recently described method (12) on a Synergy HT plate reader (Bio-Tek Instruments, Winooski, VT). The liposomes were diluted in a standardized universal buffer solution containing 11.5 mM borate, 7.8 mM citrate, 18.7 mM phosphate, 68.9 mM NaOH, adjusted to the desired pH with HCl and to 0.21 M ionic strength with NaCl (SUBS (16)) or as indicated. For experiments with SUBS containing TRIS, the pH was adjusted after the addition of TRIS. The pH was stable during all kinetic measurements. All solutions were equilibrated at 25°C. At time 0, 10–20 μl of 0.1–1 mM ACA solution were added to the wells of a 96-well plate (Corning No. 3915) containing each 200 μl of the diluted liposomes. The final lipid concentration was between 2 and 3 mg/ml, the total Tb^{3+} concentration ~0.1 mM and the ACA concentrations between 5 and 100 μM. Under these conditions the kinetics were independent of the ACA and liposome concentrations. The samples were excited at the wavelength resulting in the highest signal of the complex, i.e., between 272 and 318 nm, and Tb^{3+} luminescence was recorded every 30 s at 545 nm with a time delay of 0.05 ms, gate time of 1 ms, cycle time of 20 ms, and at 1 flash per cycle. The time delay was set to filter out any signal from other sources than Tb^{3+}. The assays were run for 1–2 h. Fast kinetics were determined with an SX18-MC stopped-flow instrument (Applied Photophysics, Leatherhead, UK) under similar conditions but without time delay.

To estimate the concentration ratio of SA in the inner and outer aqueous compartments of the Tb^{3+}-containing liposomes at $I(max)$, i.e., at the permeation equilibrium, the partitioning of ^{14}C-SA between Tb^{3+}-containing PhC liposomes and SUBS at pH 7 was determined by equilibrium dialysis as described below and compared to the partitioning in Tb^{3+}-free liposomes. The total SA concentration was 0.06 mM in the liposome-containing chamber. The ratio of the SA concentrations of the inner and outer compartments was ~1.5, the estimated association constant of a 1:1 SA-Tb^{3+} complex 10^2 M^{-1}.

Data analysis

Data were analyzed with the solver tool of Microsoft Excel:mac and with SigmaPlot. The luminescence/time curves ($I(t) = f(t)$) were fitted with a monoexponential and a biexponential function, respectively (Eqs. 1 and 2).

$$I(t) = I(max) - (I(max) - I(0))e^{-kt} \quad (1)$$

$$I(t) = I(max)_1 + I(max)_2 - ((I(max)_1 - I(0)_1)e^{-k_1 t} + (I(max)_2 - I(0)_2)e^{-k_2 t}), \quad (2)$$

where $I(max)$ denotes the maximal luminescence of the respective exponential, $I(0)$ the luminescence at time 0, i.e., the intersection with the ordinate, and k the rate constant of the respective exponential. Indices in Eq. 2 refer to the fast (index$_1$) and the slow (index$_2$) process. For the determination of permeation coefficients the biexponential Eq. 2 was used, and

apparent permeation coefficients $Perm_{app}$ were calculated from k_1 and the liposomal radius r as follows:

$$Perm_{app} = k_1 \times r/3, \quad (3)$$

where $r/3$ is used as an approximation for the ratio between the total inner aqueous volume of the liposomes and the total membrane area (17). The radius r was estimated from the hydrodynamic mean diameter of the liposomes (see above). Intrinsic permeation coefficients of the net neutral ($Perm^{N}$), mono- ($Perm^{I^-}$) and di-deprotonated ($Perm^{I^{2-}}$) compounds were fitted from the $logPerm_{app}$/pH profiles according to Eq. 4:

$$\log Perm_{app} = \log(\alpha^{N} \times 10^{\log Perm^{N}} + \alpha^{I^-} \times 10^{\log Perm^{I^-}} + \alpha^{I^{2-}} \times 10^{\log Perm^{I^{2-}}}), \quad (4)$$

where α^{N}, α^{I^-}, and $\alpha^{I^{2-}}$ are the molar fractions of the net neutral, the mono-deprotonated, and the di-deprotonated acids (18), (Eqs. 5–7):

$$\alpha^{N} = 10^{-2pH}/(10^{-2pH} + 10^{-pH-pK_a^{N/I^-}} + 10^{-pK_a^{N/I^-}-pK_a^{I^-/I^{2-}}}),$$

for DPA and

$$\alpha^{N} = 1/(1 + 10^{pH-pK_a}), \text{ for 2-OH-NA and SA} \quad (5)$$

$$\alpha^{I^-} = 10^{-pH-pK_a^{N/I^-}}/(10^{-2pH} + 10^{-pH-pK_a^{N/I^-}} + 10^{-pK_a^{N/I^-}-pK_a^{I^-/I^{2-}}}),$$

for DPA and

$$\alpha^{I^-} = 1 - \alpha^{N}, \text{ for 2-OH-NA and SA} \quad (6)$$

$$\alpha^{I^{-2}} = 10^{-pK_a^{N/I^-}-pK_a^{I^-/I^{2-}}}/(10^{-2pH} + 10^{-pH-pK_a^{N/I^-}} + 10^{-pK_a^{N/I^-}-pK_a^{I^-/I^{2-}}}), \text{ for DPA and}$$

$$\alpha^{I^{-2}} = 0, \text{ for 2-OH-NA and SA.} \quad (7)$$

The pK_a values were determined by potentiometric titration (see above).

The pH-partition hypothesis neglects $Perm^{I^-}$ and $Perm^{I2-}$ when estimating membrane permeation. To test the hypothesis for the studied ACAs, $logPerm^{N^*}$ values were extrapolated for each $logPerm_{app}$ value according to Eq. 8:

$$Perm^{N^*} = Perm_{app}/\alpha^{N}. \quad (8)$$

pH-Dependent partitioning in the liposome system

The affinity of ^{14}C-SA to liposomal membranes was determined by a standardized equilibrium dialysis system at 37°C (16). The pH was adjusted with buffer as indicated, the ^{14}C-SA concentration was 10^{-7} M and PhC concentrations were as indicated.

Distribution coefficients were calculated according to Eq. 9 (16):

$$D = (c_{LB} - c_B) \times v_{LB}/(c_B \times v_L) + 1, \quad (9)$$

where c_{LB} is the molar solute concentration in the liposome-containing chamber and c_B in the buffer chamber. The symbol v_{LB} denotes the sample volume of the liposome suspension, v_L the volume of the lipophilic phase, i.e., the lipid bilayers. This volume was calculated from the PhC concentrations in the dialysis cells, which were determined with an enzymatic choline quantification assay (19), and a density of 1.0 g/ml for the lipids.

The pH-dependent distribution of SA between the lipid bilayer and the aqueous phase was fitted as described elsewhere (20) according to Eq. 10:

$$\log D = \alpha^{N} \times 10^{\log P^{N}} + \alpha^{I^-} \times 10^{\log P^{I^-}}, \quad (10)$$

where P^{N} is the partition coefficient of the neutral and P^{I^-} of the deprotonated SA.

RESULTS

pK_a and $logP_{Octanol}$ of the tested ACAs

The pK_a and the $logP_{Octanol}$ values of the net neutral ($logP^{N}_{Octanol}$) and deprotonated ($logP^{I^-}_{Octanol}$ and $logP^{I^{2-}}_{Octanol}$) ACAs were determined by potentiometric titration as described under Methods (Table 1). The $logP^{N}_{Octanol}$ was highest for SA, i.e., 2.48, and lowest for 2-OH-NA, i.e., −0.13. Of the anions, salicylate was the least lipophilic, with a $logP^{I^-}_{Octanol}$ below the detection limit, i.e., <-1.7. The differences between $logP^{N}_{Octanol}$ and $logP^{I^-}_{Octanol}$, i.e., $\delta logP^{N/I^-}_{Octanol}$ ranged from 0.9 to >4.1 (Table 1). The $logP$ of the di-deprotonated DPA was similar to the $logP$ of the mono-anion of DPA, as no significant changes in the apparent $pK_a^{I^-/I^{2-}}$ were detected at the different n-octanol/0.15 M KCl ratios.

Kinetic analysis of the membrane permeation

To investigate the permeation kinetics, Tb^{3+}-containing liposomes were incubated with the ACAs, excited at the appropriate wavelength and the luminescence at 545 nm was recorded as described under Methods. The resulting luminescence/time curves were fitted with either a monoexponential (Eq. 1) or a biexponential (Eq. 2) function. Fig. 2 *A* shows data from a representative permeation assay with SA and egg PhC liposomes, together with the two fitted curves according to Eqs. 1 and 2. The residuals of the fits are shown in Fig. 2 *B*. The best fit with the lowest residuals was obtained with the biexponential function in all permeation assays. The maximum of the faster exponential term, $I(max)_1$, was in all permeation experiments between 30 and 50% of the total maximum, i.e., of the sum of $I(max)_1$ and $I(max)_2$. The rate constant k_1 of the faster exponential was used to calculate the apparent permeation coefficients $Perm_{app}$.

To confirm that the rate-limiting step was the permeation process and not the formation of the Tb^{3+}/SA complex, the interaction of Tb^{3+} and SA was determined at pH 7.0 in absence of liposomes under stopped-flow conditions (Fig. 2 *C*). Kinetic data were fitted with the biexponential function (Eq. 2) revealing rate constants of 6 s^{-1} (fast phase) and 0.5 s^{-1} (slow phase). The rate constant of the slow phase was six times higher than the rate constants of the fastest

TABLE 1 pK_a and *n*-octanol/0.15 M KCl partition coefficients of the studied acids

	DPA	2-OH-NA	SA
pK_a^{N/I^-}*	2.07 ± 0.08	4.97 ± 0.01	2.75 ± 0.03
$pK_a^{I^-/I^{2-}}$*	4.57 ± 0.02	–	–
$logP^{N}_{Octanol}$†	0.62 ± 0.26	−0.13 ± 0.05	2.48 ± 0.01
$logP^{I^-}_{Octanol}$†	−0.83 ± 0.50	−1.05 ± 0.11	<-1.7
$\partial logP^{N/I^-}_{Octanol}$‡	1.45	0.92	>4.1

*Mean value ± SD; $n = 3$; $T = 25$°C.
†Fitted value ± SE; $T = 25$°C.
‡$\partial logP^{N/I^-}_{Octanol} = logP^{N}_{Octanol} - logP^{I^-}_{Octanol}$.

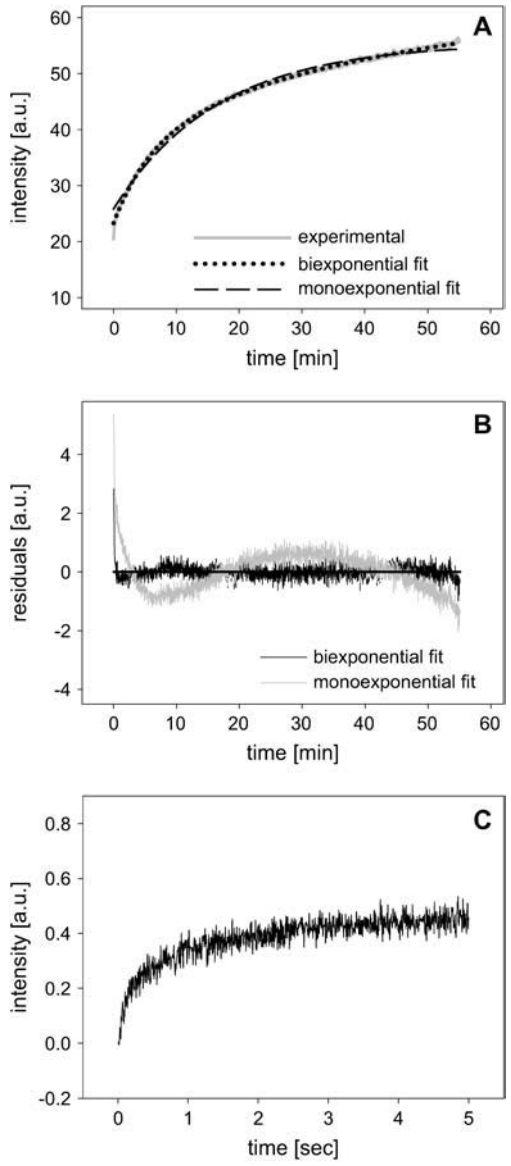

FIGURE 2 Kinetic of SA entry into egg PhC liposomes at pH 7.0. (*A*, *B*) Tb^{3+}-loaded egg PhC liposomes were incubated in SUBS, pH 7.0, and 9 μM SA (final concentration) were added at time 0. The system was excited at 318 nm and Tb^{3+} luminescence was registered at 545 nm. (*A*) Experimental luminescence/time curve and fits with a mono- and biexponential function, respectively. (*B*) Residuals of the fit functions. (*C*) Kinetics of the complex formation between Tb^{3+} and SA. Solutions of 0.5 mM $TbCl_3$ and 0.5 mM SA in 20 mM MOPS containing 0.2 M NaCl, pH 7, were mixed in a volume ratio of 10:1 with a stopped-flow apparatus and the Tb^{3+} luminescence was recorded. a.u., arbitrary units.

permeation kinetics, i.e., of 2-OH-NA at low pH in the egg PhC liposome system (0.086 s^{-1}).

pH-Dependent permeation across egg PhC bilayers

The pH-dependent permeation of the three ACAs, DPA, 2-OH-NA, and SA, across egg PhC bilayers was determined between pH ~ 3 and pH ~ 7. Permeation was not studied at pH values outside this pH range as the protonation of the PhC phosphate group below pH 3 affects drug-membrane interactions (21) and precipitation occurred during the assay above pH 7.0, probably due to the hydroxylation of Tb^{3+}. The permeation profiles are shown in Fig. 3. The three tested acids permeated slower above their pK_a^{N/I^-} than below or close to it, reaching a plateau one to two pH units above it.

The $logPerm_{app}/pH$ profiles were fitted with a Hendersson-Hasselbalch function considering all ionization species with their intrinsic permeability coefficients $logPerm^N$ for the net neutral compound, $logPerm^{I^-}$ for the mono-deprotonated acid and $logPerm^{I^{2-}}$ for the di-deprotonated DPA (Eq. 4). The fit parameters are shown in Table 2. The difference between the intrinsic *logPerm* values of two compound species differing by one proton, i.e., $\delta logPerm$ (Table 2), was highest for the pair of neutral and mono-deprotonated DPA, i.e., 2.2. The respective values for 2-OH-NA and SA were 1.1 and 1.8, i.e., the anions of the three tested acids permeated between 12 and 155 times slower than the respective net neutral species. The complete deprotonation of DPA did not reduce permeation as compared to the mono-anion. The direct comparison of the fitted permeation/pH profiles of the tested acids is shown in Fig. 3 *D*.

Beside the fits considering the permeation of all ionization species, $logPerm_{app}$/pH profiles were calculated from the fitted $logPerm^N$ values shown in Table 2 with Eq. 8, neglecting $logPerm^{I^-}$ and $logPerm^{I^{2-}}$ according to the pH-partition hypothesis. The calculated $logPerm_{app}$/pH profiles are shown in Fig. 3, *A–C*, as dashed lines. Additionally, $logPerm^{N*}$ values calculated from the experimental $logPerm_{app}$ values with Eq. 8 are shown as open triangles in the same graphs. If the pH-partition hypothesis would apply to PhC bilayer permeation, these values would be constant, i.e., pH-independent, and the dashed lines would follow the experimental data.

pH-Dependent affinity to egg PhC bilayers

To shed light on the influence of partitioning on the permeation of neutral and deprotonated SA, the pH-dependent affinity of SA to egg PhC liposomes was determined as described under Methods. Fig. 4 shows the pH-dependent partitioning and the fitted distribution profile according to Eq. 9. The fitted $logP_{PhC}^N$ and $logP_{PhC}^{I^-}$ values are shown in Table 2. The difference between the $logP_{PhC}$ values of the two ionization species, i.e., 1.6, was similar to the difference between the intrinsic *logPerm* values in the same system, i.e., 1.8. This means that the ionization of the acid reduced egg PhC bilayer affinity and permeation by similar factors, i.e., 43 and 66, respectively. It should be noted here that the permeation was determined at 25°C while partitioning was studied at 37°C.

To estimate the PhC bilayer affinity of 2-OH-NA and of DPA, which are not available radioactively labeled, the buffer

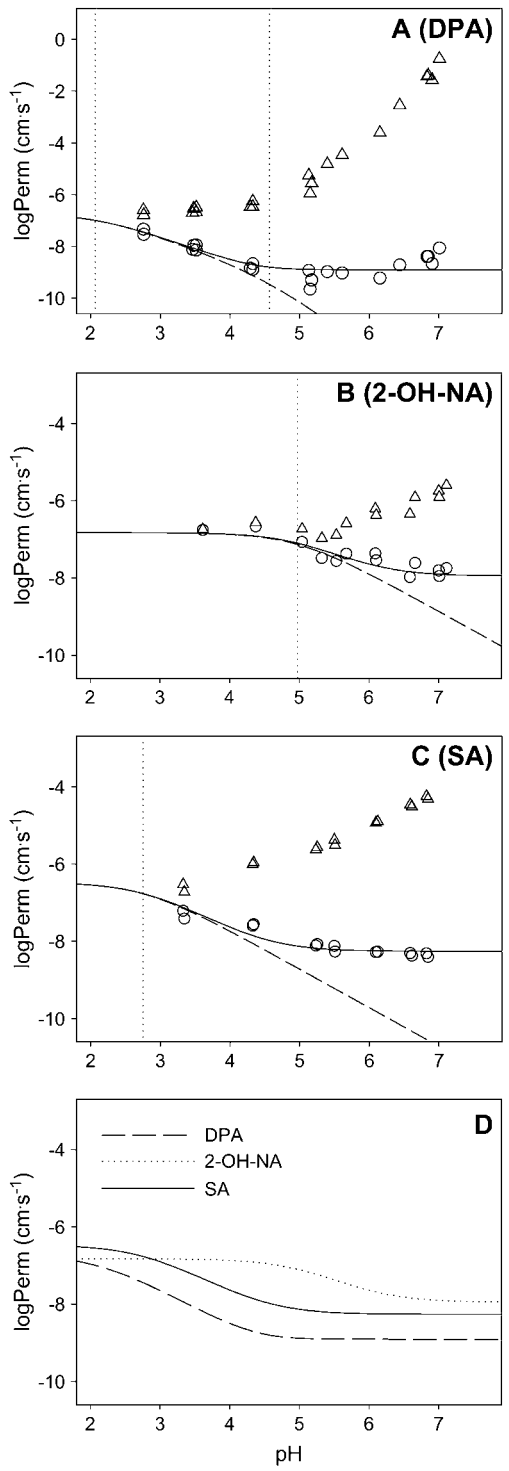

FIGURE 3 pH-Dependent permeation of DPA, 2-OH-NA, and SA across egg PhC bilayers. The $logPerm_{app}$ values (○) of DPA (*A*), 2-OH-NA (*B*), and SA (*C*) were calculated from the fast exponential term k_1 of the biexponential kinetics of liposome entry. (*A–C*) (*solid line*) $logPerm_{app}$/pH profiles were fitted with a function based on the Hendersson-Hasselbalch equation with the titrated pK_a of the respective acid (*dotted line*) and considering intrinsic permeation coefficients for each ionization species. The fitted intrinsic permeation coefficients are shown in Table 2. (*D*) Comparison of the fitted $logPerm_{app}$/pH profiles of the three acids. (*A–C*) (*dashed line*) Hypothetical $logPerm_{app}$/pH profile calculated from the fitted $logPerm^{N}$, neglecting permeation of the anion(s) (see text for details). (△) $logPerm^{N*}$ values calculated for each experimental $logPerm_{app}$ assuming that only the neutral acid contributes to permeation (see text for details). The kinetics of 2-OH-NA at pH $< pK_a$ were determined with a stopped-flow instrument. Data of each profile are from ≥2 independent experiments.

TABLE 2 Membrane affinity and membrane permeation parameters of the studied acids

	DPA	2-OH-NA	SA
$logP^{N}_{PhC}$*	n.d.†	n.d.†	2.66 ± 0.01
$logP^{I^-}_{PhC}$*	n.d.†	n.d.†	1.03 ± 0.10
$logPerm^{N}_{PhC}$ (cm×s^{-1})‡	−6.71 ± 0.19	−6.78 ± 0.08	−6.45 ± 0.10
$logPerm^{I^-}_{PhC}$ (cm×s^{-1})‡	−8.90 ± 0.55	−7.86 ± 0.09	−8.27 ± 0.05
$logPerm^{I^{2-}}_{PhC}$ (cm×s^{-1})‡	−8.90 ± 0.13	–	–
$logPerm^{N}_{DPPC}$ (cm×s^{-1})‡	n.d.	−7.90 ± 0.17	n.d.
$logPerm^{I^-}_{DPPC}$ (cm×s^{-1})‡	n.d.	−8.32 ± 0.18	n.d.
$\partial logP^{N/I}_{PhC}$§	n.d.	n.d.	1.6
$\partial logPerm^{N/I^-}_{PhC}$¶	2.2	1.1	1.8
$\partial logPerm^{N/I^-}_{DPPC}$‖	n.d.	0.4	n.d.

*Fitted value ± SE; $T = 37°C$.

†Value below detection limit.

‡Fitted value ± SE; $T = 25°C$. For DPA, the constraint $logPerm^{I^-}_{PhC} > logPerm^{I^{2-}}_{PhC}$ was set.

§$\partial logP^{N/I^-}_{PhC} = logP^{N}_{PhC} - logP^{I^-}_{PhC}$.

¶$\partial logPerm^{N/I^-}_{PhC} = logPerm^{N}_{PhC} - logPerm^{I^-}_{PhC}$.

‖$\partial logPerm_{DPPC} = logPerm^{N}_{DPPC} - logPerm^{I^-}_{DPPC}$.

n.d., not determined.

phase was spiked with Tb^{3+} after the equilibrium dialysis and the acids were quantified by fluorescence spectrometry. Due to the very low membrane affinity, no accurate $logP_{PhC}$ and $\delta logP^{N/I^-}_{PhC}$ values could be determined. The $logP^{N}_{PhC}$ of net neutral 2-OH-NA was <0.8 and of DPA <0, respectively.

Influence of counterions on the permeation

To investigate the influence of counterions on the permeation of the net neutral and deprotonated ACAs, permeation experiments were performed at pH 3.0 and pH 7.0 in either of the following buffer conditions: i), SUBS, which contains ~0.2 M Na^+; ii), 0.2 M TRIS/HCl (only pH 7.0); iii), SUBS containing 0.2 M TRIS/HCl; and iv), 0.2 M TRIS containing 0.2 M NaCl (only pH 7.0). The $Perm_{app}$ values are shown in Fig. 5. At pH 7.0, where all three ACAs are >99% deprotonated (DPA di-anionic), TRIS/HCl led to a 2.7-fold increase of the permeation coefficient of DPA and fourfold of SA as compared to SUBS, but had no influence on 2-OH-NA permeation at this pH. The effects of TRIS were independent of the presence of SUBS or NaCl in the experiments. At pH 3.0, the addition of TRIS to the SUBS increased the permeation of 2-OH-NA by a factor of ~1.4 (all $\alpha \leq 0.05$). The percentage of neutral 2-OH-NA is 98.9 at this pH. No significant effect was observed on the

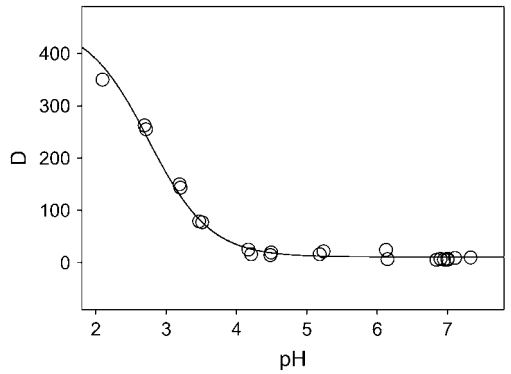

FIGURE 4 pH-Dependent affinity of SA to egg PhC bilayers. Partition coefficients of ^{14}C-SA between egg PhC bilayers (2–3 mg lipid/ml) and SUBS were determined by equilibrium dialysis. (○) Experimental *D*-values; (*solid line*) fit with a function based on the Hendersson-Hasselbalch equation with the titrated pK_a and considering the partitioning of both ionization species of SA. The fitted *logP* values are shown in Table 2.

permeation of the other two ACAs at pH 3.0. The weak increase of SA permeation at pH 3.0 in the presence of TRIS corresponds to the increase expected from the 64% anionic SA present at pH 3.0. The calculated fractions of neutral, mono-deprotonated, and di-deprotonated acids at the investigated pH values are shown in the legend of Fig. 5.

Influence of counterions on the membrane affinity

To investigate the influence of TRIS on the membrane affinity of SA, the partitioning of ^{14}C-SA was studied with egg PhC liposomes at pH ~ 7 and at pH 3.3 in: i), SUBS; ii), 0.2 M TRIS/HCl (pH 7); and iii), SUBS containing 0.2 M TRIS (pH 3.3). The resulting *D*-values are shown in Fig. 6. The membrane affinity was 1.3–1.4 times higher in the presence of TRIS than in SUBS alone at both pH values ($\alpha \leq 0.01$).

Influence of the bilayer state on the pH-dependent membrane permeation

To test whether anion permeation also occurs in the gel state of the membrane, the pH-dependent permeation of 2-OH-NA was studied with DPPC liposomes at 25°C (T_c 41°C (22)). The parameters $logPerm^N$ and $logPerm^{I^-}$ of this compound are well defined in the experimental $logPerm_{app}$/pH profile as the single pK_a value of 4.97 is ideally located between the experimental pH limits (see Fig. 3 *B*). 2-OH-NA is therefore ideal for the comparison of the pH-dependent permeation in different systems. As shown in Fig. 7 and Table 2, the anion permeation was not much slower than the permeation of the net neutral compound in the DPPC liposome system. In comparison with the egg PhC system, $Perm^N$ was ~13 times lower in the DPPC system whereas the permeation of the anion was ~2.9 times slower.

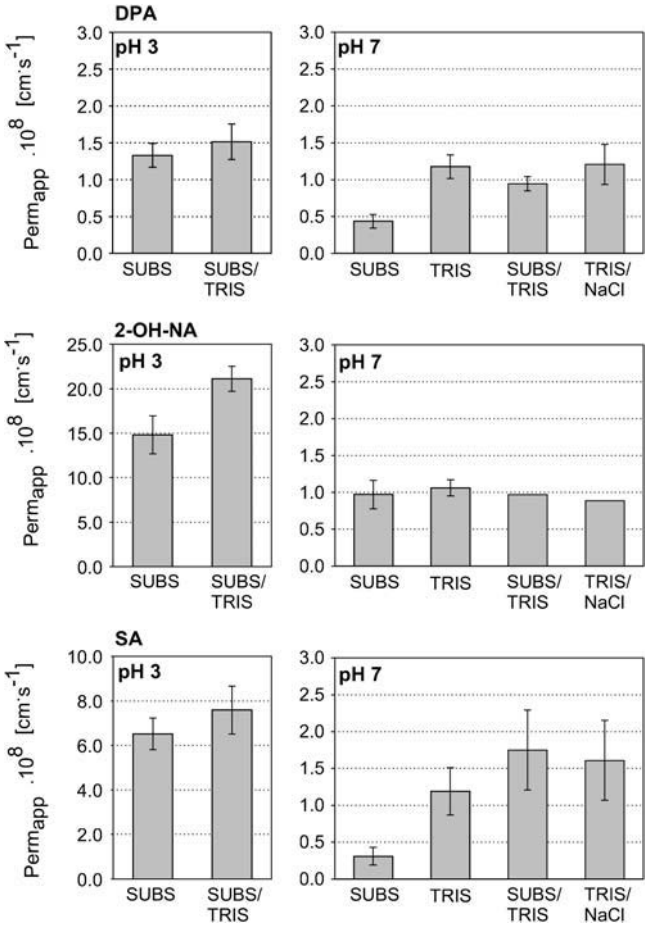

FIGURE 5 Influence of the counterion on egg PhC bilayer permeation. $Perm_{app}$ were determined at pH 7.0 and pH 3.0 with Na^+ or protonated TRIS or both as possible counterions for permeation. (*SUBS*/*TRIS*) SUBS containing 0.2 M TRIS; (*TRIS*) 0.2 M TRIS/HCl; (*TRIS*/*NaCl*) 0.2 M TRIS containing 0.2 M NaCl. The fractions of neutral/mono-anionic(/di-anionic) acids at pH 3.0 are 0.10/0.87/0.02 for DPA, 0.99/0.01 for 2-OH-NA, and 0.36/0.64 for SA. At pH 7.0 the fractions are 0.00000/0.004/0.996 for DPA, 0.009/0.991 for 2-OH-NA, and 0.00006/0.99994 for SA. Shown are mean values and standard deviations of ≥3 independent experiments or values from a single experiment (no error bars).

DISCUSSION

The kinetics of 2-OH-NA, SA, and DPA permeation across egg PhC bilayers were studied as a function of their ionization state with a recently introduced liposomal assay (12). This assay allows the direct measurement of the permeation kinetics of drug-like molecules across lipid bilayers. The prerequisite for the compound is a Tb^{3+}-chelating or ligating group, such as a carboxylic acid, coupled to an aromatic system. The permeation kinetics must be slower than the complex formation with Tb^{3+}. Applying luminescence techniques the permeant concentrations are kept in the micromolar range whereas the lipid concentration is in the millimolar range. Under these conditions, luminescence and permeation are concentration independent allowing the kinetic analysis of bilayer permeation.

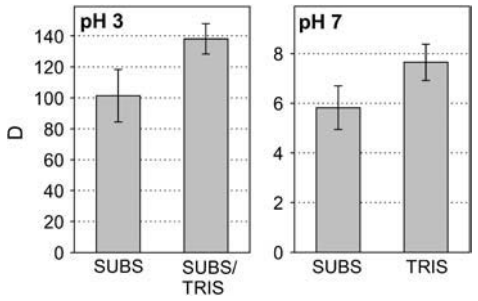

FIGURE 6 Influence of the counterion on the egg PhC membrane affinity of SA. The partitioning of ^{14}C-SA in the egg PhC liposome system was determined at pH 3.3 and at pH ~ 7 in the presence of Na^+ or TRIS or both as possible counterions for partitioning. For definitions of SUBS, SUBS/TRIS, and TRIS, see Fig. 5 legend. The lipid concentrations were 2–3 mg/ml at pH 3.3 and 50 mg/ml at pH 7. The high lipid concentration at pH 7 reduced the experimental errors of the relatively low *logD*-values in this pH range.

The fitted permeation coefficients of the three net neutral acids were in a narrow range between $logPerm^{N}_{PhC}$ −6.5 and −6.8 (cm s^{-1}). This is several magnitudes lower than the value of −0.16 (cm s^{-1}) calculated for neutral SA based on measurements with planar lipid bilayers of egg PhC/dodecane and corrected for the unstirred water layer adjacent to the membrane (23) but is similar to the value published for 4-hydroxy-methyl-hippuric acid, i.e., −6.3, determined with egg PhC liposomes applying a separation technique (24).

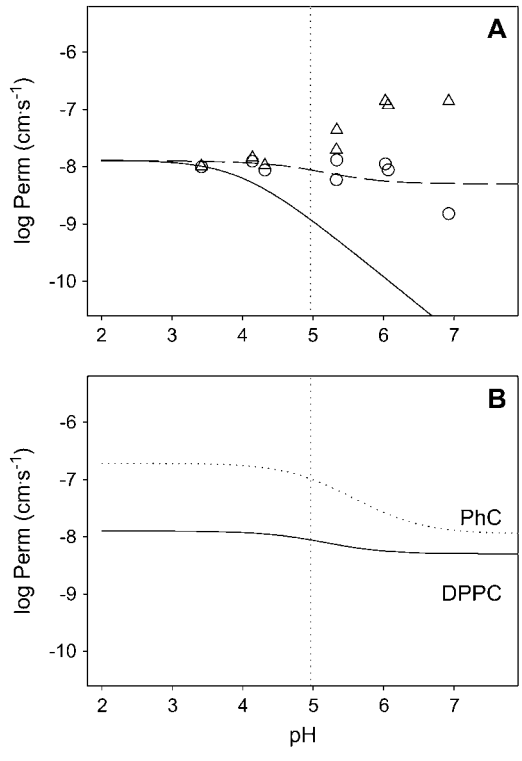

FIGURE 7 Influence of the membrane state on 2-OH-NA permeation. (*A*) $logPerm_{app}$/pH profile of 2-OH-NA in DPPC liposomes at 25°C, i.e., $<T_c$. Symbols and lines as in Fig. 3. The fitted intrinsic permeation coefficients are shown in Table 2. (*B*) Comparison of the fitted $logPerm_{app}$/pH profiles of 2-OH-NA in egg PhC liposomes (liquid crystal state, *dotted line*) and in DPPC liposomes (gel state, *solid line*).

The permeation of the deprotonated acids across egg PhC bilayers is by several magnitudes faster than expected from the pH-partition hypothesis, which assumes negligible permeation of the charged species as compared to the neutral one (10,25). In our study, the ratios between the permeation coefficients of the net neutral species and the anions were 12, 66, and 155 for 2-OH-NA, SA, and DPA, respectively. For comparison, Males and Herring (26) found a ratio of 14 between the permeation coefficients of neutral and deprotonated glycolic acid in an NMR study.

According to Eq. 4, the permeation of a base is controlled by the permeation of the ion in the pH range $<$ (pK_a − $\delta logPerm^{N/I^-}$) and of an acid in the pH range $>$ (pK_a + $\delta logPerm^{N/I^-}$). In other words, if the ratio of the concentrations of ions and neutral species at a particular pH is higher than the ratio of $Perm^N/Perm^{I^-}$ at the same pH, the ions contribute more to total permeation than the neutral species. If the product of $Perm^{I^-}$ and the molar fraction of the anion is equal to the product of $Perm^N$ and the molar fraction of the neutral species, permeation is determined to equal extents by the two species. Considering the small $\delta logPerm^{N/I^-}_{PhC}$ values determined in this study, this leads to significantly higher permeation at physiological pH than expected from the pH-partition hypothesis and $logPerm^N$. At physiological pH, i.e., pH 7.4, the permeation of all three tested acids is fully controlled by their anions whereas the permeation of the neutral species is negligible. The calculation of the $logPerm^{N*}$ values at each experimental pH assuming zero permeation of the anions, illustrates how this assumption can lead to erroneous estimates of $logPerm^N$. Preliminary results from five additional derivatives of benzoic acid revealed the same picture: the plateaus defined by the permeation of the anions in the *logPerm*/pH profiles ($logPerm^{I^-}$) started at pH $<$ 7 and permeation at pH 7 was completely controlled by the anions of the tested acids (A. V. Thomae, H. Wunderli-Allenspach, and S. D. Krämer, unpublished data).

The lower ratio between the permeation coefficients of the net neutral and anionic species of 2-OH-NA and SA as compared to DPA could be due to their potential to form an intramolecular hydrogen bond between the deprotonated acid group and the β-hydroxyl group leading to a delocalization of the charge. The fully deprotonated species of DPA has no potential to form intramolecular hydrogen bonds and the charges of the di-anion cannot delocalize at all. We expected that DPA would follow the pH-partition hypothesis due to the above-mentioned characteristics of the di-anion. However, even under these conditions, the ratio between $Perm^N$ and $Perm^{I^-}$ was only 155, i.e., 2.2 orders of magnitude and permeation at pH 7 was completely controlled by the di-anion.

Membrane permeation is determined by the partition rate constants between the lipid leaflet and the aqueous environment and the flip-flop rate constants between the two lipid leaflets in the bilayer. The flip-flop is supposed to be rate limiting in the permeation process (27). In this case, permeation is determined by the partition coefficient between the lipid and the aqueous phases and the flip-flop rate constant (4). The difference between the $logPerm^{N}_{PhC}$ and $logPerm^{I^-}_{PhC}$ of SA in the egg PhC liposome system was similar to the difference of the respective $logP^{N}_{PhC}$ and $logPerm^{I^-}_{PhC}$, i.e., 1.8 and 1.6, respectively. This indicates that the translocation rate constant of the deprotonated acid is in the same range as that of the neutral molecule and that the difference in permeation of the two ionization species is mainly given by their difference in membrane affinity. This is in contrast to the general assumption that charged species avoid the acyl chain region of the bilayer resulting in negligible translocation (10,11). Further studies on the temperature dependence of the partitioning and permeation of neutral and charged ACAs are needed to draw a final conclusion on the influence of the ionization state on membrane affinity and flip-flop rates.

Ion-pair partitioning was described by Austin et al. (28) and Avdeef et al. (29). In biphasic systems relatively lipophilic counterions can lead to higher partition coefficients than hydrophilic ions. To study the influence of the counterion on the permeation of the tested ACAs, the SUBS buffer was replaced or supplemented by TRIS and permeation was determined at pH 3.0 and 7.0, respectively. The TRIS cation (the protonated base) is more lipophilic than the Na^+ ion and would therefore be more effective as a counterion for ion-pair permeation of the tested ACAs. The influence of TRIS on the permeation of the three compounds was not consistent. TRIS enhanced the permeation of the deprotonated DPA and SA. This is in accordance with the ion-pair partition hypothesis. However, the permeation enhancing effect of TRIS on net neutral but not on deprotonated 2-OH-NA would not be expected from this hypothesis. These data show that counterions have an influence on lipid bilayer permeation, however, the effect can not be predicted from the ion-pair partition hypothesis or from the effect on the affinity of the permeant to the membrane. In addition to their influence on partitioning and permeation, buffer ions could also influence the physicochemical properties of the lipid bilayer.

The relatively high permeation coefficients of the anions as compared to the net neutral acids could be related to the fluidity of the membrane and to the formation of dynamic pores in the liquid crystal bilayer (30). To investigate the influence of the bilayer state on ion permeation, the pH-dependent permeation kinetics of 2-OH-NA were studied in the DPPC liposome system. At 25°C, DPPC bilayers are in the gel state resulting in a more rigid membrane (31) and a significantly lower occurrence of dynamic pores (30,32) compared to the liquid crystal state. The permeation coefficient of the neutral species was 13 times lower than in the egg PhC liposome system. However, $\delta logPerm^{N/I^-}_{DPPC}$ was smaller than the difference in the egg PhC liposome system and $Perm^{I^-}$ was only 2.9 times lower in the gel state than in the liquid crystal state. If anion permeation would depend on dynamic pores in the liquid crystal state we would expect much lower $Perm^{I^-}$ values in the gel state. As the ratio of neutral/anion permeation was even smaller in the gel state than in the liquid crystal state, we conclude that the unexpectedly low ratio of permeation of net neutral and charged species in the egg PhC liposome system is not related to the fluidity of the bilayer or to the formation of dynamic pores. In addition, pores allowing ACA anion exchange would possibly also result in a higher Tb^{3+} leakage than observed in our studies. The fact that the membrane state and/or the saturation level of the acyl chains affect the permeation of the two ionization species to different extents points to divergent permeation processes. A thermodynamic analysis will disclose more details.

The permeation of a solute across a lipid bilayer is generally estimated from its lipophilicity, expressed as the partition coefficient in the 1-octanol/water system. We found no strong correlation between $logPerm^{N}_{PhC}$ and $logP^{N}_{Octanol}$ for the three studied acids. The $logPerm^{N}_{PhC}$ values of the three ACAs did not differ significantly whereas $logP^{N}_{Octanol}$ ranged from -0.1 to 2.5. The ratios between the partition coefficient of the neutral and the mono-anionic species of 2-OH-NA and DPA were in a similar range as the ratios of their permeation coefficients, i.e., 8.3 and 28. However, it was $>10^4$ for SA (5.6×10^3 in a previous study (33)). This implicates that the ionization of SA has a far higher effect on the partitioning between water and 1-octanol than on the permeation across egg PhC bilayers. Considering solvatochromic comparison methods according to el Tayar et al. (34) or Abraham and Chadha (35), the lack of relationship could be due to different effects of the physicochemical characteristics such as molecular volume, dipolarity/polarizability, and hydrogen-bond donor and acceptor capacities on the partitioning of the solutes between water and 1-octanol and the partitioning and permeation out of water into and across an egg PhC bilayer. Further studies with a larger series of ACAs are currently performed in our laboratory to unravel the relation between lipid bilayer permeation and physicochemical parameters.

All permeation kinetics were best fitted with a biexponential function. The biexponential shape was pH-independent, was also found with DPPC liposomes, i.e., in the gel state, and was independent of the buffer system. As the faster exponential reached 30–50% of the maximal luminescence intensity and was determinant for the initial slope of the kinetics, it was used for the calculation of $Perm_{app}$. The biphasic permeation kinetics could be related to the biphasic kinetics of the complex formation as observed in the absence of liposomes. To exclude any artifacts, the following controls were carried out. A simulation was performed to test

whether the fast phase is due to translocation without desorption from the inner lipid leaflet and the slow phase to the desorption step. In this case the ratio of the luminescence maxima of the two exponentials would be pH-dependent as for instance the ratio of membrane located to aqueous SA is ~30 times higher at pH 3 than at pH 7. However, this was not the case in our study. Furthermore, the presence of either two permeation mechanisms or of two populations of liposomes or permeants could lead to a biexponential kinetic. The coexistence of dimers or higher aggregates and monomers in the aqueous phase (36) or in the membrane would cause a concentration-dependent kinetic and this was not observed in our study. To rule out an influence of potentially multilamellar liposomes, kinetics with liposomes after different numbers of extrusion passages were compared. The passage number had no influence on the kinetics in our study (data not shown).

The universal buffer solution SUBS was used to cover a wide pH range. As Tb^{3+} is complexed by citrate, precipitates with phosphate, both components of SUBS, and shows no ACA-induced increase in luminescence in the presence of SUBS, the buffer was only added to the final liposomes. Under these conditions the lipid bilayer separated Tb^{3+} from the extraliposomal aqueous phase containing the buffer ions. The separation was maintained during all experiments, i.e., for several hours. This, together with the evaluation of the permeation system shown elsewhere (12), corroborates that the increase in luminescence is directly linked to ACA permeation and not to Tb^{3+} leakage or liposome disintegration. Despite the absence of buffer ions in the liposomal lumen, no significant pH shift is expected upon different permeation of the neutral and anionic species. The pH-equilibration in egg PhC liposomes occurs with a half-life of ~1–2 min (16). This is faster than the experimental permeation half-life values with the exception of 2-OH-NA permeation $\leq$ pH 5.1. In the latter case, a pH shift would not exceed 0.05 pH units (except for the data point at pH 5.1), as the proton concentrations were $\geq$10 times higher than the ACA concentrations in this pH range.

Due to their small molecular size, the three tested acids could cross intestinal epithelia mainly via the paracellular route (37). In this case, bilayer permeation would not be relevant for the in vivo absorption. However, we took advantage of the relatively slow permeation of these small size molecules to analyze the permeation kinetics over a broad pH range and to scrutinize the permeation coefficients of the neutral and the anionic species. The aim of this study is to better understand bilayer permeation, which is one single relevant mechanism of in vivo barrier passage. Understanding the single mechanisms will finally lead to a better understanding of in vivo barrier passage.

In contrast to our findings with the egg PhC liposomes, permeation of SA across PhC/dodecane impregnated filter membranes (PAMPA) followed the pH-partition hypothesis (38) and permeation was controlled by the neutral species at pH 7. The discrepancy between the two systems could be based on the characteristics of the barriers. In our study, we measure lipid bilayer permeation whereas the PAMPA experiments determine diffusion across a solution of lipids in dodecane. PAMPA is a well-established high-throughput in vitro permeation model to estimate the in vivo barrier passage of drug candidates with a much higher capacity than the described liposomal assay. The latter, in turn, provides profound insight into lipid bilayer permeation, which will finally contribute to the improvement of predictive in vitro and in silico models.

Ongoing work focuses on the influence of the lipid composition, in particular cholesterol and negatively charged phospholipids, on the permeation behavior of ACAs, and on the correlations between permeation coefficients, membrane affinities, and physicochemical parameters of the permeants. The thermodynamic analysis of the permeation profiles should shed light on the processes involved in membrane permeation.

In conclusion, deprotonated ACAs permeate egg PhC and DPPC bilayers by several magnitudes faster than expected from the pH-partition hypothesis. At physiological pH, the permeation of DPA, 2-OH-NA, and SA is fully controlled by the anions.

We thank Manuel Morillas Díaz for the introduction to the stopped-flow technique, Selina Decurtins and Christine Klötzer for their experimental contributions, and Maja Günthert for carefully reading the manuscript.

REFERENCES

1. van de Waterbeemd, H., and E. Gifford. 2003. ADMET in silico modelling: towards prediction paradise? *Nat. Rev. Drug Discov.* 2:192–204.
2. Di, L., and E. H. Kerns. 2003. Profiling drug-like properties in discovery research. *Curr. Opin. Chem. Biol.* 7:402–408.
3. Kennedy, T. 1997. Managing the drug discovery/development interface. *Drug Discov. Today.* 2:436–444.
4. Krämer, S. D. 2005. Lipid bilayers in ADME: permeation barriers and distribution compartments. *In* Pharmacokinetic Profiling in Drug Research: Biological, Physicochemical and Computational Strategies. B. Testa, S. D. Krämer, H. Wunderli-Allenspach, and G. Folkers, editors. Wiley-VCH, Weinheim, Germany.
5. Faller, B., and F. Wohnsland. 2001. Physicochemical parameters as tools in drug discovery and lead optimization. *In* Pharmacokinetic Optimization in Drug Research: Biological, Physicochemical and Computational Strategies. B. Testa, H. van de Waterbeemd, G. Folkers, and R. Guy, editors. Wiley-VCH, Weinheim, Germany.
6. Genty, M., G. Gonzalez, C. Clere, V. Desangle-Gouty, and J.-Y. Legendre. 2001. Determination of the passive absorption through the rat intestine using chromatographic indices and molar volume. *Eur. J. Pharm. Sci.* 12:223–229.
7. Bermejo, M., A. Avdeef, A. Ruiz, R. Nalda, J. A. Ruell, O. Tsinman, I. Gonzalez, C. Fernandez, G. Sanchez, T. M. Garrigues, and V. Merino. 2004. PAMPA: a drug absorption in vitro model. 7. Comparing rat in situ, Caco-2, and PAMPA permeability of fluoroquinolones. *Eur. J. Pharm. Sci.* 21:429–441.
8. Malkia, A., L. Murtomaki, A. Urtti, and K. Kontturi. 2004. Drug permeation in biomembranes: in vitro and in silico prediction and

influence of physicochemical properties. *Eur. J. Pharm. Sci.* 23: 13–47.

9. Krämer, S. D. 2001. Liposome/water partitioning: theory, techniques and applications. *In* Pharmacokinetic Optimization in Drug Research: Biological, Physicochemical and Computational Strategies. B. Testa, H. van de Waterbeemd, G. Folkers, and R. Guy, editors. VHCA and Wiley-VCH, Zurich, Switzerland and Weinheim, Germany. 401–428.
10. Yu, L. X., E. Lipka, J. R. Crison, and G. L. Amidon. 1996. Transport approaches to the biopharmaceutical design of oral drug delivery systems: prediction of intestinal absorption. *Adv. Drug Del. Rev.* 19: 359–376.
11. Youdim, K. A., A. Avdeef, and N. J. Abbott. 2003. In vitro trans-monolayer permeability calculations: often forgotten assumptions. *Drug Discov. Today.* 8:997–1003.
12. Krämer, S. D., and H. Wunderli-Allenspach. 2003. No entry for TAT(44–57) into liposomes and intact MDCK cells: novel approach to study membrane permeation of cell-penetrating peptides. *Biochim. Biophys. Acta.* 1609:161–169.
13. Avdeef, A. 1993. Refinement of partition coefficients and ionization constants of multiprotic substances. *J. Pharm. Sci.* 82:183–190.
14. Krämer, S. D., J.-C. Gautier, and P. Saudemon. 1998. Considerations on the potentiometric log P determination. *Pharm. Res.* 15:1310–1313.
15. Hope, M. J., M. B. Bally, G. Webb, and P. R. Cullis. 1985. Production of large unilamellar vesicles by a rapid extrusion procedure. Characterization of size distribution, trapped volume and ability to maintain a membrane potential. *Biochim. Biophys. Acta.* 812:55–65.
16. Pauletti, G. M., and H. Wunderli-Allenspach. 1994. Partition coefficients in vitro: artificial membranes as a standardized distribution model. *Eur. J. Pharm. Sci.* 1:273–282.
17. Paula, S., A. Volkov, and D. Deamer. 1998. Permeation of halide anions through phospholipid bilayers occurs by the solubility-diffusion mechanism. *Biophys. J.* 74:319–327.
18. Martin, A., P. Bustamante, and A. H. C. Chun. 1993. Physical Pharmacy. Lea & Febiger, Philadelphia, PA.
19. Ottiger, C., and H. Wunderli-Allenspach. 1999. Immobilized artificial membrane (IAM)-HPLC for partition studies of neutral and ionized acids and bases in comparison with the liposomal partition system. *Pharm. Res.* 16:643–650.
20. Marenchino, M., A. L. Alpstäg-Wöhrle, B. Christen, H. Wunderli-Allenspach, and S. D. Krämer. 2004. α-Tocopherol influences the lipid membrane affinity of desipramine in a pH-dependent manner. *Eur. J. Pharm. Sci.* 21:313–321.
21. Krämer, S. D., C. Jakits-Deiser, and H. Wunderli-Allenspach. 1997. Free fatty acids cause pH-dependent changes in drug-lipid membrane interactions around physiological pH. *Pharm. Res.* 14:827–832.
22. Marsh, D. 1990. CRC Handbook of Lipid Bilayers. CRC Press, Boca Raton, FL.
23. Gutknecht, J., and D. C. Tosteson. 1973. Diffusion of weak acids across lipid bilayer membranes: effects of chemical reactions in the unstirred layers. *Science.* 182:1258–1261.
24. Mayer, P. T., T. X. Xiang, and B. D. Anderson. 2000. Independence of substituent contributions to the transport of small molecule permeants in lipid bilayers. *AAPS PharmSci.* 2:E14.
25. Frezard, F., and A. Garnier-Suillerot. 1991. DNA-containing liposomes as a model for the study of cell membrane permeation by anthracycline derivatives. *Biochemistry.* 30:5038–5043.
26. Males, R. G., and F. G. Herring. 1999. A 1H-NMR study of the permeation of glycolic acid through phospholipid membranes. *Biochim. Biophys. Acta.* 1416:333–338.
27. Gennis, R. B. 1989. Biomembranes: Molecular Structure and Function. C. R. Cantor, editor. Springer, New York, NY.
28. Austin, R. P., P. Barton, A. M. Davis, C. N. Manners, and M. C. Stansfield. 1998. The effect of ionic strength on liposome-buffer and 1-octanol-buffer distribution coefficients. *J. Pharm. Sci.* 87:599–607.
29. Avdeef, A., K. J. Box, and K. Takacs-Novak. 1995. pH-Metric log P. 6. Effects of sodium, potassium, and N-CH_3-D-glucamine on the octanol-water partitioning of prostaglandins E_1 and E_2. *J. Pharm. Sci.* 84:523–529.
30. Jansen, M., and A. Blume. 1995. A comparative study of diffusive and osmotic water permeation across bilayers composed of phospholipids with different head groups and fatty acyl chains. *Biophys. J.* 68:997–1008.
31. New, R. R. C., V. Torchillin, and V. Weissig. 2003. Liposomes (Practical Approach Series). D. Rickwood and B. D. Hames, editors. Oxford University Press, Oxford, UK.
32. Lawaczeck, R. 1988. Defect structures in membranes: routes of the permeation of small molecules. *Ber. Bunsenges. Phys. Chem.* 92:961–963.
33. Ottiger, C. 1998. Partition behaviour of acids, bases and neutral drugs with liposomes, IAM-HPLC and 1-octanol. PhD thesis. ETH Swiss Federal Institute of Technology, Zurich, Switzerland.
34. el Tayar, N., T. Ruey-Shiuan, B. Testa, P.-A. Carrupt, and A. Leo. 1991. Partitioning of solutes in different solvent systems: the contribution of hydrogen-bonding capacity and polarity. *J. Pharm. Sci.* 80: 590–598.
35. Abraham, M. H., and H. S. Chadha. 1996. Applications of a solvation equation to drug transport properties. *In* Lipophilicity in Drug Action and Toxicology. V. Pliska, B. Testa, and H. van de Waterbeemd, editors. VCH Verlagsgesellschaft mbH, Weinheim, Germany. 311–337.
36. Kleinfeld, A. M., P. Chu, and J. Storch. 1997. Flip-flop is slow and rate limiting for the movement of long chain anthroyloxy fatty acids across lipid vesicles. *Biochemistry.* 36:5702–5711.
37. Obata, K., K. Sugano, R. Saitoh, A. Higashida, Y. Nabuchi, M. Machida, and Y. Aso. 2005. Prediction of oral drug absorption in humans by theoretical passive absorption model. *Int. J. Pharm.* 293: 183–192.
38. Ruell, J. A., K. L. Tsinman, and A. Avdeef. 2003. PAMPA: a drug absorption in vitro model. 5. Unstirred water layer in iso-pH mapping assays and pKa(flux)-optimized design (pOD-PAMPA). *Eur. J. Pharm. Sci.* 20:393–402.